

# Direct observation of microtubule dynamics at kinetochores in *Xenopus* extract spindles: implications for spindle mechanics

Paul Maddox,<sup>1,2</sup> Aaron Straight,<sup>1,3</sup> Peg Coughlin,<sup>1,3</sup> Timothy J. Mitchison,<sup>1,3</sup> and Edward D. Salmon<sup>1,2</sup>

<sup>1</sup>Cell Division Group, Marine Biological Laboratory, Woods Hole, MA 02543

<sup>2</sup>Department of Biology, University of North Carolina, Chapel Hill, Chapel Hill, NC 27599

<sup>3</sup>Department of Cell Biology, Harvard Medical School, Boston, MA 02115

Microtubule plus ends dynamically attach to kinetochores on mitotic chromosomes. We directly imaged this dynamic interface using high resolution fluorescent speckle microscopy and direct labeling of kinetochores in *Xenopus* extract spindles. During metaphase, kinetochores were stationary and under tension while plus end polymerization and poleward microtubule flux (flux) occurred at velocities varying from 1.5–2.5  $\mu\text{m}/\text{min}$ . Because kinetochore microtubules polymerize at metaphase kinetochores, the primary source of kinetochore tension must be the spindle forces that produce flux and not a kinetochore-based mechanism. We infer that the kinetochore resists translocation of kinetochore micro-

tubules through their attachment sites, and that the polymerization state of the kinetochore acts a “slip-clutch” mechanism that prevents detachment at high tension. At anaphase onset, kinetochores switched to depolymerization of microtubule plus ends, resulting in chromosome-to-pole rates transiently greater than flux. Kinetochores switched from persistent depolymerization to persistent polymerization and back again during anaphase, bistability exhibited by kinetochores in vertebrate tissue cells. These results provide the most complete description of spindle microtubule poleward flux to date, with important implications for the microtubule–kinetochore interface and for how flux regulates kinetochore function.

## Introduction

During mitosis, kinetochore fibers produce force that stretches centromere chromatin and pulls chromosomes poleward. In tissue culture cells, poleward movement appears to be generated mainly by kinetochore-based force-generating mechanisms coupled to depolymerization of microtubules at kinetochore plus end attachment sites (the “Pac-Man” mechanism; for review see Inoue and Salmon, 1995; Mitchison and Salmon, 2001). Kinetochores in cultured cells also exhibit anti-poleward movement, coupled to polymerization of microtubule plus ends at kinetochores (“Pac-Man in reverse”). Likewise, kinetochores in cultured cells often oscillate between persistent phases of poleward and anti-poleward movement, behavior termed “directional instability” (Skibbens et al., 1993). Attached kinetochores in budding yeast also exhibit directional instability, suggesting that depolymerization and

polymerization states of kinetochores are widely conserved throughout evolution (He et al., 2000; Pearson et al., 2001).

Another source of poleward force at attached kinetochores is poleward movement (flux) of kinetochore microtubules (Mitchison, 1989; Desai et al., 1998). Poleward flux is translocation of tubulin polymer poleward coupled to minus end depolymerization near the spindle poles (Mitchison 1989). Flux may act as a “traction fiber” mechanism for aligning chromosomes to the metaphase plate, generating tension at kinetochores for inactivating the spindle checkpoint and contributing to anaphase segregation of chromosomes (Kapoor and Compton, 2002). Spindle microtubules that exhibit poleward flux also exhibit “treadmilling” in a plus-to-minus direction when their plus ends are polymerizing (Grego et al., 2001).

In tissue culture cells, kinetochore-based mechanisms appear to make the dominant contribution to chromosome movement because kinetochore microtubule flux is slow ( $\sim 0.5 \mu\text{m}/\text{min}$ ) compared with the velocities of kinetochore poleward and anti-poleward movements (1.5–2.5  $\mu\text{m}/\text{min}$ ; Rieder and

Abbreviation used in this paper: FSM, fluorescent speckle microscopy.

The online version of this article includes supplemental material.

Address correspondence to E.D. Salmon, Dept. of Biology, CB3280, University of North Carolina, Chapel Hill, Chapel Hill, NC 27599. Tel.: (919) 962-2354. Fax: (919) 962-1625. email: tsalmon@email.unc.edu

Key words: kinetochore; fluorescent speckle microscopy; mitosis; centromere; anaphase

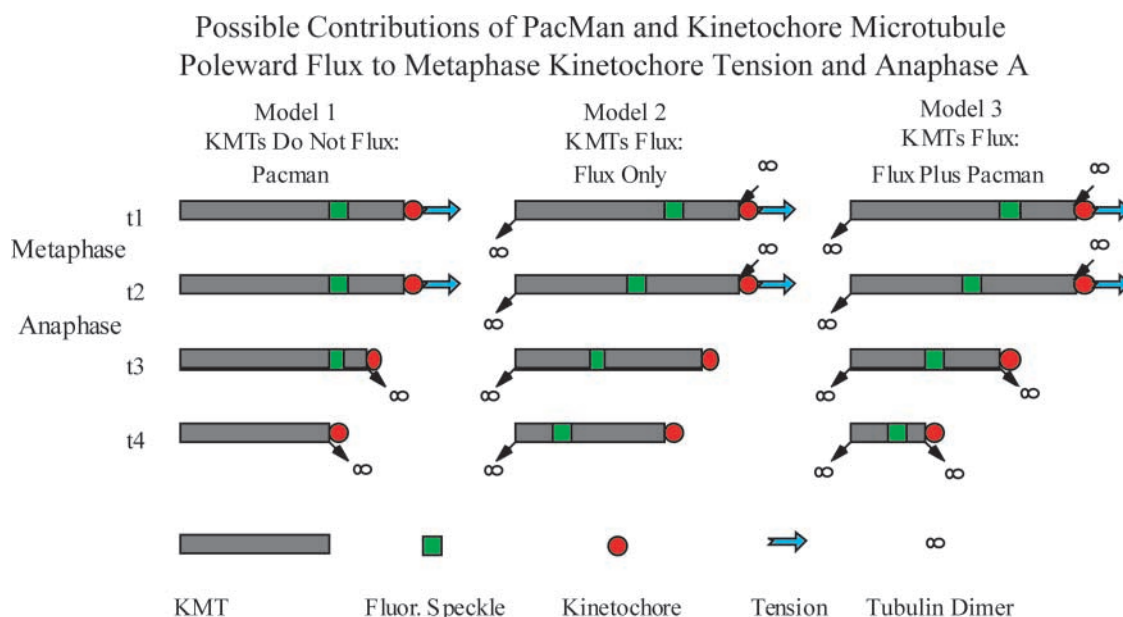


**Figure 1. Three models based on different contributions of kinetochole motility and kinetochole microtubule flux to metaphase kinetochole tension and anaphase A.** For each model, only a single kinetochole microtubule (KMT) is shown with the polar minus end (–) at the left and the plus end (+) attached to the kinetochole on the right. Arrows indicate sites of polymerization or depolymerization. Metaphase includes sequential times, t1 and t2; anaphase onset occurs at t2 and continues for sequential times t2, t3, and t4. At metaphase, the centromeric linkage between sister kinetocholes and polar ejection forces on the arms support tension at kinetocholes (large blue arrow). Tension is lost at anaphase onset when sisters separate and the polar ejection forces on the arms are inactivated (Funabiki and Murray, 2000). See text for details.

Salmon, 1998). In *Xenopus* egg extract spindles, flux mechanisms appear dominant because spindle microtubules exhibit average flux rates near the average rate of anaphase A velocity ( $\sim 2.0 \mu\text{m}/\text{min}$ ; Desai et al., 1998). Similarly, in *Drosophila* embryo mitotic spindles, flux is fast, implying that traction fiber mechanics represent a major component of anaphase A movement (Brust-Mascher and Scholey, 2002; Maddox et al., 2002).

In *Xenopus* and *Drosophila* spindles, where flux is fast, metaphase kinetocholes do not exhibit directional instability (Desai et al., 1998; Maddox et al., 2002). Chromosomes in spermatocytes, oocytes, early embryos, and higher plants also do not exhibit kinetochole oscillations. Fig. 1 shows three possible models that could explain both the lack of metaphase chromosome oscillations and the mechanism of anaphase A seen in the systems just mentioned.

In model 1, there is no flux of kinetochole microtubules. This is a possibility because kinetochole microtubules were not absolutely discriminated from the great majority of non-kinetochole microtubules in the previous analyses of flux in *Xenopus* extract spindles and *Drosophila* spindles during metaphase and early anaphase (Desai et al., 1998; Brust-Mascher and Scholey, 2002; Maddox et al., 2002). At metaphase, kinetocholes pull on microtubules by Pac-Man mechanisms, but are stalled by tension between sister kinetocholes and for unknown reasons do not oscillate. In anaphase, loss of centromere tension from disjunction allows kinetocholes to move poleward coupled to plus end depolymerization. Model 2 is of historical significance because it is similar to mechanisms suggested by Inoue and Salmon (1995) and the treadmilling model proposed by Margolis and Wilson (1981) (for review see Mitchison and Salmon, 2001), and conclusions from

more recent flux measurements by Desai et al. (1998) for *Xenopus* extract spindles. This model is based solely on flux. At metaphase, polymerization at kinetocholes occurs at the flux rate, whereas in anaphase, polymerization stops at kinetocholes. Kinetocholes then become tightly bound to the microtubule lattice (“park” state), and are pulled poleward by flux. Model 3 predicts that both kinetochole motility and flux contribute to metaphase alignment and anaphase A. At metaphase, the kinetochole is biased by flux into persistent polymerization, whereas sister separation at anaphase onset allows kinetocholes to switch to depolymerization and increase the rate of anaphase A to velocities greater than flux. This is the conclusion reached in recent experiments in *Drosophila*, but it is based on the unproven assumption that kinetochole microtubules flux at the rate of nonkinetochole microtubules (Brust-Mascher and Scholey, 2002; Maddox et al., 2002).

To test these possibilities and other fundamental aspects of the microtubule–kinetochole interface, we used high resolution fluorescent speckle microscopy (FSM) methods (Maddox et al., 2002, 2003) to directly image microtubule polymerization/depolymerization at kinetocholes relative to flux during metaphase and anaphase in spindles assembled in *Xenopus* egg extracts. Our results show that model 3 is correct, and we discuss the implications of rapid poleward flux for spindle mechanics at the microtubule–kinetochole interface.

## Results and discussion

### Direct observation of microtubule dynamics at kinetocholes

Metaphase spindles with replicated chromosomes in *Xenopus* egg extracts (Desai et al., 1998) were labeled with a

low level of X-rhodamine tubulin to produce fluorescent speckled microtubules (Waterman-Storer et al., 1998; Fig. S1, available at <http://www.jcb.org/cgi/content/full/jcb.200301088/DC1>), and also with a nonperturbing fluorescent antibody directed to the inner kinetochore protein CENP-A. Fig. 2 A shows one frame from a time-lapse sequence where optical sections were recorded at 10-s intervals using spinning-disk confocal microscopy. The open arrow in Fig. 2 A points to one pair of sister kinetochores kept in focus during the movie sequence. Note that spinning-disk confocal imaging resolved bundles of microtubules attached to kinetochores as well as bundles of nonkinetochore microtubules that pass by the chromosomes at the equator, and microtubule fluorescent speckles within these fibers (see also Fig. S1 and Video 1). Kinetochore microtubule bundles contain gaps in fluorescence between the plus ends of sister kinetochore fibers; gaps were absent in adjacent interpolar microtubule bundles (closed arrow). In electron micrographs, kinetochores exhibit a trilaminar structure with attached bundles of microtubules, typical of vertebrates (Fig. S2; Rieder and Salmon, 1998).

#### At metaphase, kinetochore microtubule flux occurs at slightly slower velocities compared with nonkinetochore microtubules

To test if polymerization occurs at kinetochores of metaphase chromosomes, we generated kymographs of speckle movements along aligned kinetochore fibers (Fig. 2 B).

The analysis showed that fluorescent speckles appeared at kinetochores and moved poleward with a constant velocity of  $2.0 \pm 0.5 \mu\text{m}/\text{min}$  ( $n = 72$ ). This result eliminates model 1.

During the analysis period, the distance between chromosomes and spindle poles changed little, allowing comparisons between rates of poleward flux in kinetochore fiber microtubules and in adjacent interpolar microtubule bundles. Fig. 2 C shows a kymograph of a nonkinetochore microtubule bundle (Fig. 2 A, closed arrow; Video 2) adjacent to the kinetochore fiber analyzed (Fig. 2 A, open arrow). Note that flux is bidirectional in the interpolar microtubule bundle near the spindle equator and unidirectional in kinetochore fibers. Fig. 2 D shows a histogram of kinetochore and nonkinetochore microtubule flux velocities relative to stationary kinetochores. Average values measured for the poleward flux of nonkinetochore microtubules was  $2.3 \pm 0.6 \mu\text{m}/\text{min}$  ( $n = 113$ ). The 10% lower average rate of poleward flux of kinetochore microtubules relative to nonkinetochore microtubules was statistically different based on a *t* test ( $P = 0.004$ ). This suggests that kinetochores impose a small load on flux during metaphase, although it is possible that the CENP-A antibody bound to the kinetochore slightly perturbs kinetochore function.

#### At metaphase, poleward flux creates tension at kinetochores

The stretch of the centromere between sister kinetochores measures tension at metaphase kinetochores (Waters et al.,

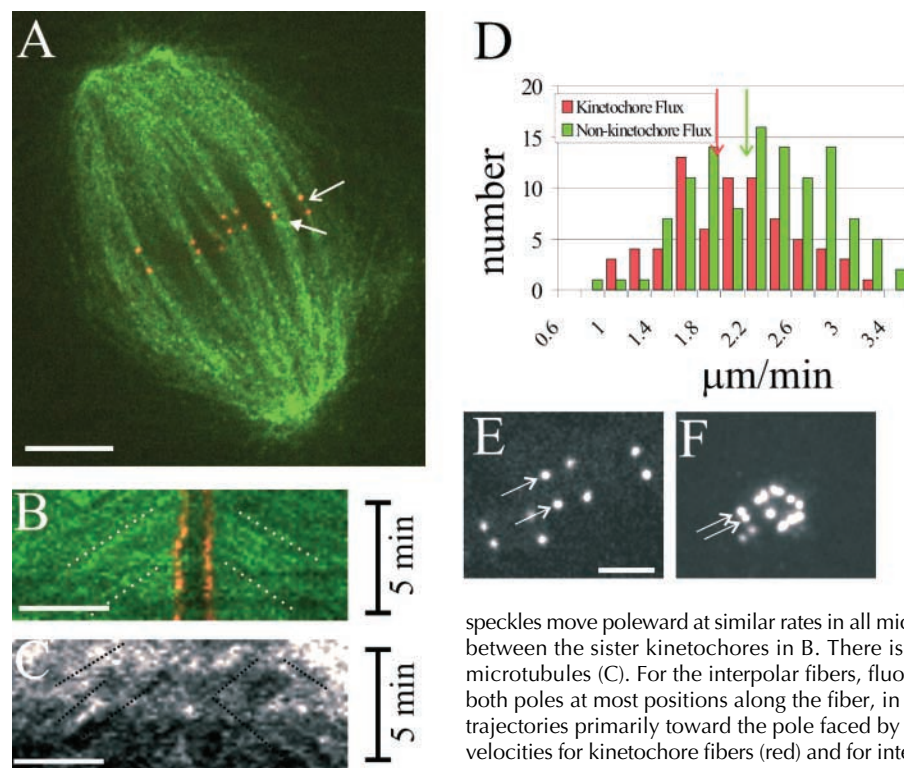


**Figure 2. Confocal FSM of microtubule polymerization at metaphase kinetochores and centromere stretch.**

(A) Selected frame from a time-lapse movie showing the polymerization at kinetochores labeled with fluorescent CENP-A antibodies (red) and the poleward flux of kinetochore microtubule fluorescent speckles (green). The open arrow marks a kinetochore pair that was aligned for kymograph analysis (see Materials and Methods); closed arrow marks a nonkinetochore fiber. (B) Kymograph of the kinetochore pair marked with open arrow in A. The kinetochores move relatively little with respect to each other while speckles on microtubules appear at the kinetochores and flux poleward. Flux velocity is proportional to the slope of the speckle trajectories away from the vertical direction in B. (C) Kymograph of nonkinetochore microtubules shows that

speckles move poleward at similar rates in all microtubules. Note the gap of tubulin fluorescence between the sister kinetochores in B. There is no such gap for the interpolar bundles of microtubules (C). For the interpolar fibers, fluorescent speckle trajectories are seen toward both poles at most positions along the fiber, in contrast to kinetochore fibers, which exhibit trajectories primarily toward the pole faced by the kinetochore. D shows a histogram of flux velocities for kinetochore fibers (red) and for interpolar spindle fibers (green) obtained from the slopes of kymographs such as those in B and C. Note they have a similar distribution, with nonkinetochore flux being slightly faster. Colored arrows point to average values (see text). Image of sister kinetochores labeled with fluorescent CENP-A antibody in unfixed extracts at metaphase (E) or where spindles were disassembled with  $10 \mu\text{M}$  nocodazole (F). Bars: A–C,  $5 \mu\text{m}$ ; E and F,  $2 \mu\text{m}$ .

1996). In metaphase spindles, the average separation of sister kinetochores marked by CENP-A antibodies was  $1.5 \pm 0.4 \mu\text{m}$  ( $n = 26$ ; Fig. 2 E). In comparison, when microtubules were completely depolymerized by  $10 \mu\text{M}$  nocodazole, sister separation was  $0.6 \pm 0.1 \mu\text{m}$  ( $n = 20$ ; Fig. 2 F). Thus, metaphase centromeres were stretched between sister kinetochores to 2.5 times their rest length.

Because microtubule plus ends polymerize at metaphase kinetochores, the primary source of kinetochore tension must be the spindle mechanisms that produce microtubule poleward flux and not a kinetochore-based mechanism. We infer that the kinetochore resists translocation of kinetochore microtubules through their attachment sites as a function of translocation velocity and the molecular viscosity of attachment (Howard, 2001). The idea that microtubule binding sites within the kinetochore produce molecular friction to a moving microtubule lattice was conceptualized by Hill (1985). The resistance at polymerizing kinetochores may be generated by transient linkages between dimers in the microtubule lattice and motor or non-motor linker molecules within the kinetochore outer plate (see diagram in Fig. 4).

### In anaphase, kinetochores switch from polymerization to depolymerization, increasing the rate of anaphase A above flux

Anaphase was initiated (Desai et al., 1998) and time-lapse series were recorded (Video 3) to test if *Xenopus* kinetochores pull their chromosomes poleward along stationary kinetochore microtubules (Fig. 1, model 1), become parked on the lattice of fluxing kinetochore microtubules (Fig. 1, model 2) or switch to depolymerization while flux persists (Fig. 1, model 3). Kymographs generated through aligned kinetochores and kinetochore fibers (Fig. 3, A and B) allowed measurement of polymerization (speckle slopes away from kinetochores) versus depolymerization (speckle slopes toward kinetochores) of microtubule plus ends at kinetochores (Fig. 3 C). Because the position of the right-hand sister kinetochore in Fig. 3 A was fixed in the alignment procedure, it appears as a vertical line in the kymograph, and the sister moved to the left after anaphase onset. In Fig. 3 B, the left-hand kinetochore was fixed, resulting in the sister moving to the right during anaphase. When sister chromosomes separated at anaphase onset, polymerization at the kinetochore slowed. When polymerization was slow enough, fluorescent speckles on kinetochore microtubules abruptly switched to movement toward the kinetochore, indicating microtubule depolymerization at kinetochores (Fig. 3, A and B). The velocity of plus end depolymerization added to the velocity of microtubule poleward flux, resulting in transient anaphase A rates greater than that of poleward flux. Variable switching between persistent polymerization and persistent depolymerization was observed for many kinetochores (Fig. 3 A). This switching likely accounts for the periods of fast and slow velocity seen in plots of kinetochore-to-pole movement, and likely explains why kinetochores move, on average,  $\sim 40\%$  faster than poleward flux of kinetochore microtubules in anaphase (Fig. 3, C and D). Only rarely and for brief periods did we see kinetochores appear to become fixed

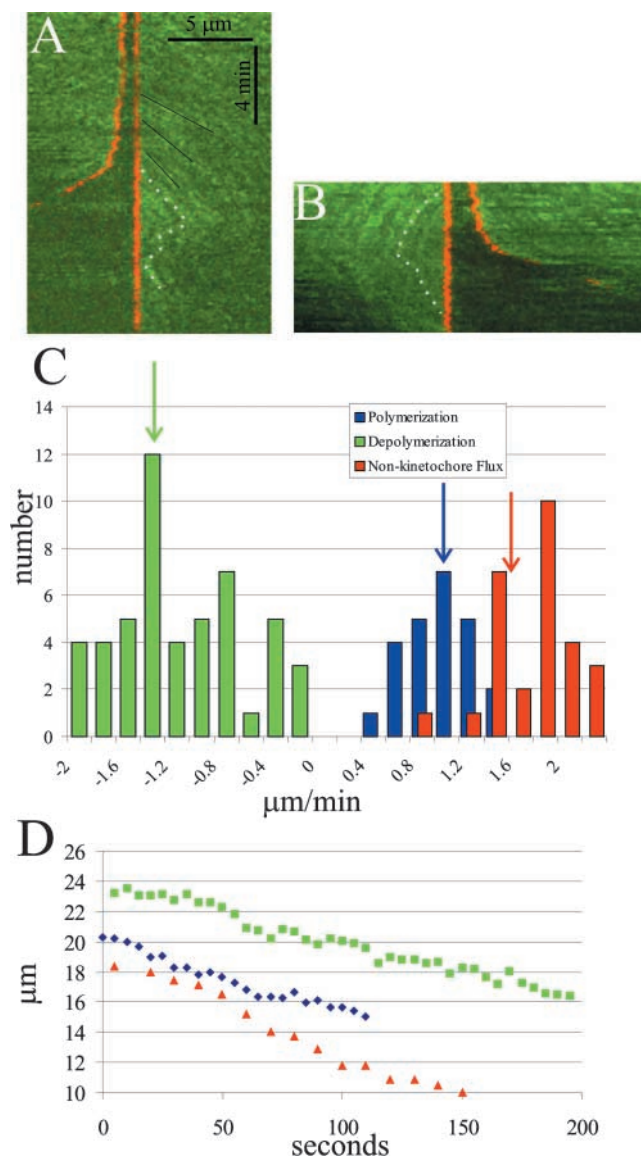


**Figure 3. Confocal FSM of microtubule polymerization/depolymerization at anaphase kinetochores.** Time-lapse images were aligned so that a selected kinetochore was fixed in position relative to the rest of the spindle (see text). A and B are kymographs made from two different aligned spindles. Dotted white lines in each kymograph highlight speckle movements relative to the aligned kinetochores. In both examples, polymerization at the kinetochores slows as sisters begin to separate in anaphase (e.g., slopes of black lines in A become more vertical). When polymerization is slow enough, the kinetochore switches to depolymerization, where speckles are seen to move toward and disappear at the kinetochores. The kinetochore in A persists in depolymerization, whereas the kinetochore in B switches back to polymerization during the interval analyzed. (C) Histograms of velocities measured for polymerization and depolymerization at kinetochores and flux during anaphase. Arrows mark the average values. Depolymerization =  $1.2 \pm 0.6 \mu\text{m}/\text{min}$  ( $n = 27$ ); polymerization =  $0.9 \pm 0.3 \mu\text{m}/\text{min}$  ( $n = 24$  measurements); flux =  $1.6 \pm 0.4 \mu\text{m}/\text{min}$  ( $n = 27$ ). We were unable to obtain values as chromosomes approached their poles because of the curvature of the kinetochore fibers. (D) Poleward movements of three kinetochores during the first two thirds of anaphase A. Notice that the kinetochores exhibit asynchronous periods of fast and slow movement. The average velocity over this period was  $2.4 \mu\text{m}/\text{min}$  ( $n = 20$  kinetochores from six spindles).

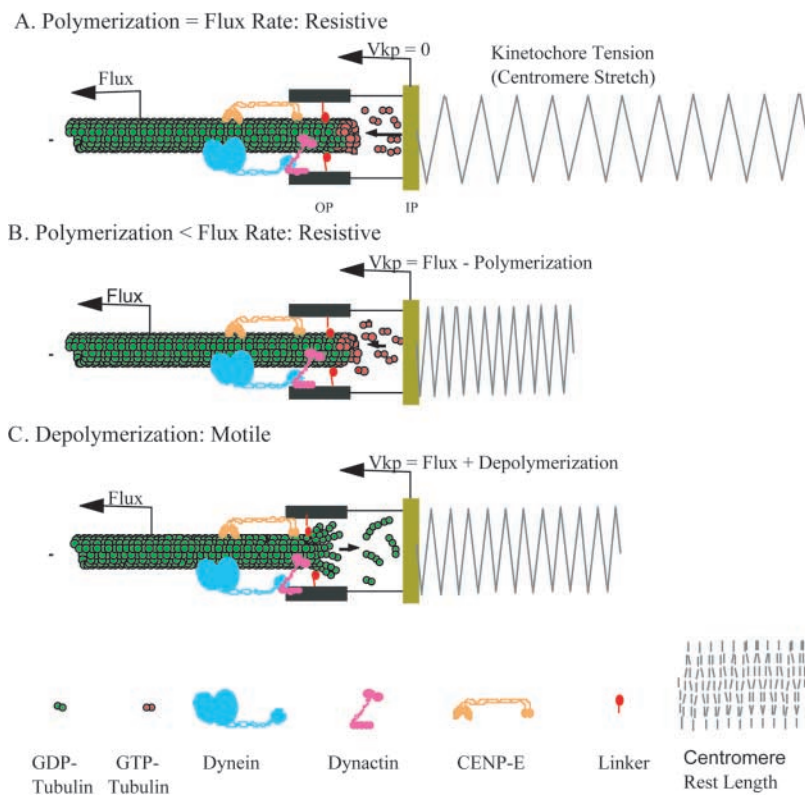


Figure 4. **Updated models for the kinetochore-microtubule interface that include contributions from flux.** Drawings in A–C are modified from Rieder and Salmon (1998). OP is a cross section of one microtubule attachment site in the outer plate of the kinetochore, and IP is a cross section of the inner plate. The stretch of the centromere beyond its rest length indicates the tension generated. Microtubule attachment and resistance to translocation through the attachment site may be provided by the microtubule motors CENP-E and cytoplasmic dynein, the nonmotor microtubule-binding domain of CENP-E, the microtubule binding domain of the p150 component of the dynactin complex bound to dynein, and unknown microtubule-binding proteins within the attachment site (see text for details).

in position at the ends of their kinetochore microtubules in anaphase. Thus, model 3 is correct and the hypothetical park state does not play a significant role in spindle mechanics in this system.

A notable observation was the distinctly bimodal distribution of polymerization/depolymerization rates at kinetochores in anaphase. We believe that this observation reflects the nature of the force-velocity relationship for kinetochores, providing fundamental insights into kinetochores as molecular engines. It suggests that the kinetochore-microtubule attachment site has two stable states of force production, and it can switch between either spontaneously or in response to applied force. The “polymerizing” state is not a neutral state (Rieder and Salmon, 1998), but a resistive, or frictional state, coupled to polymerization and plus end-directed movement (Fig. 4, A and B). Our data show that when polymerization equals flux, the kinetochore is stationary, but when sisters initially separate at anaphase onset, polymerization becomes slower than flux and the kinetochore moves poleward at a velocity given by the rate of flux minus the rate of polymerization at the kinetochore (Fig. 3 C and Fig. 4 B). Note that kinetochore resistive tension is high at metaphase when polymerization and the rate of translocation of the lattice through the attachment site equals flux (Fig. 4 A). Resistive tension becomes lower in early anaphase as sisters separate and the rate of polymerization and translocation through the attachment site decreases (Fig. 4 B). The “depolymerizing” state is the actively pulling, motile state, coupled to depolymerization and minus end-directed movement (Fig. 4 C). Fig. 3 C is the most direct and quantitative data to date supporting the idea that kinetochores are fundamentally bistable, exhibiting persistent po-

lymerization and depolymerization states, and that bistability is a property of plus end dynamic instability (Skibbens et al., 1993; Tirnauer et al., 2002; Fig. 4). Our observation of underlying kinetochore bistability in a system where chromosomes do not oscillate in metaphase points to a conserved property that is probably fundamental to kinetochore mechanochemistry.

### Implications for spindle mechanics

We suggest that kinetochores rarely park on the microtubule lattice in any system; rather, they are inherently bistable, switching between a force-generating depolymerizing state and a more passive, friction-generating polymerization state due to the fundamental mechanochemistry of the kinetochore-microtubule interface. Different spindles appear to vary considerably in the rate of flux, ranging from probably zero in yeast (Mallavarapu et al., 1999; Maddox et al., 2000) to slow in vertebrate somatic cells (for review see Desai et al., 1998) to a large fraction of anaphase A in meiotic and embryonic systems (Desai et al., 1998; Brust-Mascher and Scholey, 2002; Maddox et al., 2002). We believe that fundamentally conserved kinetochores behave differently in the three types of system as a response to this differing flux rate. At metaphase, we propose that chromosome oscillations occur for lower (but not higher) microtubule flux rates, because only high flux rates produce sufficient kinetochore tension to prevent kinetochores from switching to depolymerization (Skibbens et al., 1993). We also suggest that the polymerization state of the kinetochore represents a “slip-clutch” safety mechanism that prevents strong force from pulling plus ends out of their kinetochore attachment sites during chromosome congression or segregation. The slip-

ping clutch at the kinetochore allows the system to reduce the force on chromosomes if there is a mechanical problem.

## Materials and methods

### Labeled tubulins, labeled antibodies, and preparation of *Xenopus* extract spindles

Labeling of tubulin using X-rhodamine was performed as described previously (Waterman-Storer et al., 1998). For assaying flux, labeled tubulin was initially diluted into CSF extract 1:50, and that extract was diluted into experimental extract by 1:50 for confocal FSM. Antibodies to *Xenopus* Cenp-A were prepared and fluorescently labeled as described in the supplemental materials.

### FSM

FSM was performed using diffraction-limited spinning-disk confocal fluorescence microscopy as described in detail in Maddox et al. (2002, 2003), and with a 100×/1.4 NA Plan Apochromat objective (Nikon) with 2 × 2 binning in the cooled CCD camera (model ER; Hamamatsu Corporation). MetaMorph® software (Universal Imaging Corp.) was used to control shutters, wavelength selection, image acquisition, and storage. Sequential images of different fluorophores were acquired at 3–15-s intervals, depending on the experiment. Paired images from different color channels were within 0.5 s of each other.

### Data analysis

Measurements of the movement of fluorescent speckles and the leading edge of kinetochores relative to the spindle poles was mainly performed by hand tracking their positions or from kymographs using MetaMorph® software as described previously (Maddox et al., 2002). Kinetochore and speckle-to-pole movements were measured from the margin of the structure being analyzed to the end of the spindle fibers. Speckles were chosen for analysis based on the speckle remaining visible for at least five consecutive time points. “Custom Align” and “Rotation” algorithms in MetaMorph® were used to align spindles throughout the time-series stack of images to a given point (e.g., a single kinetochore). Color overlays were used for both kymograph methods to compare movements of microtubule fluorescent speckles to kinetochores. Velocities were obtained from the slopes of the speckle or leading-edge trajectories in the kymograph images. Statistical analysis and graphs were done in Excel (Microsoft).

### Online supplemental material

Online supplemental materials consist of materials and methods for EM and antibody production. Also included is a figure comparing wide-field imaging to confocal imaging and a figure showing thin-section EM of *Xenopus* extract kinetochores. Three movies corresponding to Fig. 2 and Fig. 3 are also included. Online supplemental material available at <http://www.jcb.org/cgi/content/full/jcb.200301088/DC1>.

We thank other members of the Cell Division Group at the Marine Biological Laboratory (Woods Hole, MA) including Arshad Desai, Tarun Kapoor, Karen Oegema, Jennifer Tirnauer, Chris Field, Andrew Murray, Lisa Cameron, and Julie Canman.

We appreciate support from the Universal Imaging Corporation, Hamamatsu Corporation, and Nikon Instruments, as well as National Institutes of Health grants GM24364 and GM606780 to E.D. Salmon and grant GM39565 to T.J. Mitchison.

Submitted: 22 January 2003

Accepted: 10 June 2003

## References

- Brust-Mascher, I., and J.M. Scholey. 2002. Microtubule flux and sliding in mitotic spindles of *Drosophila* embryos. *Mol. Biol. Cell.* 13:3967–3975.
- Desai, A., P.S. Maddox, T.J. Mitchison, and E.D. Salmon. 1998. Anaphase A chromosome movement and poleward spindle microtubule flux occur at similar rates in *Xenopus* extract spindles. *J. Cell Biol.* 141:703–713.
- Funabiki, H., and A.W. Murray. 2000. The *Xenopus* chromokinesin Xkid is essential for metaphase chromosome alignment and must be degraded to allow anaphase chromosome movement. *Cell.* 102:411–424.
- Grego, S., V. Cantillana, and E.D. Salmon. 2001. Microtubule treadmilling in vitro investigated by fluorescence speckle and confocal microscopy. *Biophys. J.* 81:66–78.
- He, X., S. Asthana, and P.K. Sorger. 2000. Transient sister chromatid separation and elastic deformation of chromosomes during mitosis in budding yeast. *Cell.* 101:763–775.
- Hill, T. 1985. Theoretical problems related to the attachment of microtubules to kinetochores. *Proc. Natl. Acad. Sci. USA.* 82:4404–4408.
- Howard, J. 2001. Mechanics of motor proteins and the cytoskeleton. Sinauer Associates, Sunderland, Massachusetts. 367 pp.
- Inoue, S., and E.D. Salmon. 1995. Force generation by microtubule assembly/disassembly in mitosis and related movements. *Mol. Biol. Cell.* 6:1619–1640.
- Kapoor, T.M., and D.A. Compton. 2002. Searching for the middle ground: mechanisms of chromosome alignment during mitosis. *J. Cell Biol.* 157:551–556.
- Maddox, P.S., K.S. Bloom, and E.D. Salmon. 2000. The polarity and dynamics of microtubule assembly in the budding yeast *Saccharomyces cerevisiae*. *Nat. Cell Biol.* 2:36–41.
- Maddox, P., A. Desai, K. Oegema, T.J. Mitchison, and E.D. Salmon. 2002. Poleward microtubule flux is a major component of spindle dynamics and anaphase A in mitotic *Drosophila* embryos. *Curr. Biol.* 12:1670–1674.
- Maddox, P.S., B. Moree, J.C. Canman, and E.D. Salmon. 2003. A spinning disk confocal microscope system for rapid high-resolution, multimode, fluorescence speckle microscopy and green fluorescent protein imaging in living cells. *Methods Enzymol.* 360:597–617.
- Mallavarapu, A., K. Sawin, and T. Mitchison. 1999. A switch in microtubule dynamics at the onset of anaphase B in the mitotic spindle of *Schizosaccharomyces pombe*. *Curr. Biol.* 9:1423–1426.
- Margolis, R.L., and L. Wilson. 1981. Microtubule treadmills—possible molecular machinery. *Nature.* 293:705–711.
- Mitchison, T.J. 1989. Polewards microtubule flux in the mitotic spindle: evidence from photoactivation of fluorescence. *J. Cell Biol.* 109:637–652.
- Mitchison, T.J., and E.D. Salmon. 2001. Mitosis: a history of division. *Nat. Cell Biol.* 3:E17–E21.
- Pearson, C.G., P.S. Maddox, E.D. Salmon, and K. Bloom. 2001. Budding yeast chromosome structure and dynamics during mitosis. *J. Cell Biol.* 152:1255–1266.
- Rieder, C.L., and E.D. Salmon. 1998. The vertebrate cell kinetochore and its roles during mitosis. *Trends Cell Biol.* 8:310–318.
- Skibbens, R.V., V.P. Skeen, and E.D. Salmon. 1993. Directional instability of kinetochore motility during chromosome congression and segregation in mitotic newt lung cells: a push-pull mechanism. *J. Cell Biol.* 122:859–875.
- Tirnauer, J.S., J.C. Canman, E.D. Salmon, and T.J. Mitchison. 2002. EB1 targets to kinetochores with attached, polymerizing microtubules. *Mol. Biol. Cell.* 13:4308–4316.
- Waterman-Storer, C.M., A. Desai, J.C. Bulinski, and E.D. Salmon. 1998. Fluorescent speckle microscopy, a method to visualize the dynamics of protein assemblies in living cells. *Curr. Biol.* 8:1227–1230.
- Waters, J.C., T.J. Mitchison, C.L. Rieder, and E.D. Salmon. 1996. The kinetochore microtubule minus-end disassembly associated with poleward flux produces a force that can do work. *Mol. Biol. Cell.* 7:1547–1558.